excitation not only provides energy required for the reaction but also gives rise to a proper adiabatic pathway that accesses the dynamical resonances in the high-energy region, whereas translational energy cannot provide such a pathway. The results presented here show that vibrationally excited molecular reactions provide a unique context for probing dynamical resonances in chemical reactions when the vibrationally adiabatic potential, which correlates to the vibrationally excited state of the reagent in the entrance channel, supports quasibound resonance states.

References and Notes

1. J. C. Polanyi, *Acc. Chem. Res.* **5**, 161–168 (1972).
2. A. Sinha, M. C. Hsiao, F. F. Crim, *J. Chem. Phys.* **92**, 6333 (1990).
3. F. F. Crim, *Acc. Chem. Res.* **32**, 877–884 (1999).
4. M. J. Bronikowski, W. R. Simpson, B. Girard, R. N. Zare, *J. Chem. Phys.* **95**, 8647 (1991).
5. R. N. Zare, *Science* **279**, 1875–1879 (1998).
6. G. C. Schatz, M. C. Colton, J. L. Grant, *J. Phys. Chem.* **88**, 2971–2977 (1984).
7. W. R. Simpson, T. P. Rakitzis, S. A. Kandel, A. J. Orr-Ewing, R. N. Zare, *J. Chem. Phys.* **103**, 7313 (1995).
8. J. P. Camden, H. A. Bechtel, D. J. Brown, R. N. Zare, *J. Chem. Phys.* **123**, 134301 (2005).
9. S. Yoon, S. Henton, A. N. Zivkovic, F. F. Crim, *J. Chem. Phys.* **116**, 10744 (2002).
10. S. Yan, Y.-T. Wu, B. Zhang, X.-F. Yue, K. Liu, *Science* **316**, 1723–1726 (2007).
11. W. Zhang, H. Kawamata, K. Liu, *Science* **325**, 303–306 (2009).
12. F. Wang, J.-S. Lin, K. Liu, *Science* **331**, 900–903 (2011).
13. G. Czakó, J. M. Bowman, *J. Am. Chem. Soc.* **131**, 17534–17535 (2009).
14. G. Czakó, J. M. Bowman, *Science* **334**, 343–346 (2011).
15. Z. Zhang, Y. Zhou, D. H. Zhang, G. Czakó, J. M. Bowman, *J. Phys. Chem. Lett.* **3**, 3416–3419 (2012).
16. G. C. Schatz, *Science* **288**, 1599–1600 (2000).
17. F. Fernández-lonso, R. N. Zare, *Annu. Rev. Phys. Chem.* **53**, 67–99 (2002).
18. K. Liu, *Annu. Rev. Phys. Chem.* **52**, 139–164 (2001).
19. K. Liu, *Adv. Chem. Phys.* **149**, 1 (2012).
20. G. C. Schatz, J. M. Bowman, A. Kuppermann, *J. Chem. Phys.* **58**, 4023 (1973).
21. S.-F. Wu, B. R. Johnson, R. D. Levine, *Mol. Phys.* **25**, 839–856 (1973).
22. D. M. Neumark *et al.*, *J. Chem. Phys.* **82**, 3067 (1985).
23. D. M. Neumark, A. M. Wodtke, G. N. Robinson, C. C. Hayden, Y. T. Lee, *J. Chem. Phys.* **82**, 3045 (1985).
24. D. E. Manolopoulos *et al.*, *Science* **262**, 1852–1855 (1993).
25. R. T. Skodje *et al.*, *Phys. Rev. Lett.* **85**, 1206–1209 (2000).
26. M. Qiu *et al.*, *Science* **311**, 1440–1443 (2006).
27. Z. Ren *et al.*, *Proc. Natl. Acad. Sci. U.S.A.* **105**, 12662–12666 (2008).
28. X. Yang, D. H. Zhang, *Acc. Chem. Res.* **41**, 981–989 (2008).
29. W. Dong *et al.*, *Science* **327**, 1501–1502 (2010).
30. D. Neuhauser *et al.*, *Science* **257**, 519–522 (1992).
31. N. Mukherjee, R. N. Zare, *J. Chem. Phys.* **135**, 024201 (2011).
32. N. V. Vitanov, M. Fleischhauser, B. W. Shore, K. Bergmann, *Adv. At. Mol. Opt. Phys.* **46**, 55–190 (2001).
33. N. Mukherjee, W. Dong, J. A. Harrison, R. N. Zare, *J. Chem. Phys.* **138**, 051101 (2013).
34. T. Wang, T. G. Yang, C. L. Xiao, D. X. Dai, X. M. Yang, *J. Phys. Chem. Lett.* **4**, 368–371 (2013).
35. R. T. Skodje, R. Sadeghi, H. Koppel, J. L. Krause, *J. Chem. Phys.* **101**, 1725 (1994).

Acknowledgments: This work was supported by the National Natural Science Foundation of China, the Ministry of Science and Technology of China, and the Chinese Academy of Sciences.

Supplementary Materials

www.sciencemag.org/content/342/6165/1499/suppl/DC1
Supplementary Text
Figs. S1 to S6
References (*36*–*39*)

27 September 2013; accepted 20 November 2013
10.1126/science.1246546

Unexpected Stable Stoichiometries of Sodium Chlorides

Weiwei Zhang,[1,2]*† Artem R. Oganov,[2,3,4]*† Alexander F. Goncharov,[5,6] Qiang Zhu,[2] Salah Eddine Boulfelfel,[2] Andriy O. Lyakhov,[2] Elissaios Stavrou,[5] Maddury Somayazulu,[5] Vitali B. Prakapenka,[7] Zuzana Konôpková[8]

Sodium chloride (NaCl), or rocksalt, is well characterized at ambient pressure. As a result of the large electronegativity difference between Na and Cl atoms, it has highly ionic chemical bonding (with 1:1 stoichiometry dictated by charge balance) and B1-type crystal structure. By combining theoretical predictions and diamond anvil cell experiments, we found that new materials with different stoichiometries emerge at high pressures. Compounds such as Na_3Cl, Na_2Cl, Na_3Cl_2, $NaCl_3$, and $NaCl_7$ are theoretically stable and have unusual bonding and electronic properties. To test this prediction, we synthesized cubic and orthorhombic $NaCl_3$ and two-dimensional metallic tetragonal Na_3Cl. These experiments establish that compounds violating chemical intuition can be thermodynamically stable even in simple systems at nonambient conditions.

At ambient conditions, NaCl is the only known stable compound in the Na-Cl system, the chemistry of which is well understood. Extreme conditions, such as high pressure, change the chemical properties of the elements, including Na and Cl (*1*, *2*), and the pressure × volume term in the free energy becomes greater than energy of chemical bonds. Thus, strongly compressed matter may exist in totally counterintuitive chemical regimes. Although unexpected high-pressure phenomena may be present in planetary systems or lead to novel exotic materials, we still lack a consistent fundamental understanding of even seemingly simple binary systems such as Na-Cl.

The high-pressure behavior of NaCl has been extensively studied experimentally at pressures up to 304 GPa (*3*–*6*) and by ab initio simulations (*7*–*9*), and very simple behavior was observed: At 30 GPa, the rocksalt structure was found to transform into the CsCl (B2-type) structure (*6*, *8*). From the Herzfeld criterion, metallization of NaCl is expected to occur at 300 GPa (*10*), whereas density functional theory calculations (*9*) suggest 584 GPa.

To find stable Na-Cl compounds and their structures that may not have been possible to observe experimentally or computationally, we used the ab initio evolutionary algorithm USPEX (*11*–*14*), which can simultaneously find stable stoichiometries and the corresponding structures in multicomponent systems (*15*). In these calculations, any combinations of numbers of atoms in the unit cell were allowed (with the total number ≤16), and calculations were performed at pressures of 1 atm, 20 GPa, 100 GPa, 150 GPa, 200 GPa, and 250 GPa. Detailed enthalpy calculations for the most stable structures allowed us to reconstruct the *P*-*x* phase diagram of the Na-Cl system (Fig. 1 and figs. S1 and S2).

To verify these predictions, we performed high-pressure experiments in a laser-heated diamond anvil cell at 10 to 80 GPa on the Na-Cl system in the presence of excess chlorine and sodium (*15*). We specifically targeted the synthesis of Na_3Cl and $NaCl_3$, which were predicted to become stable at the lowest pressures. The reaction products were examined by visual observations, optical absorption spectroscopy and Raman confocal spectroscopy, and by synchrotron x-ray diffraction (XRD) probes at room temperature (*15*).

The calculated phase diagram features unexpected compounds: $NaCl_3$, stable above 20 GPa; $NaCl_7$, stable above 142 GPa; and Na_3Cl_2, Na_2Cl, and Na_3Cl, which are stable above 120 GPa, 100 GPa, and 77 GPa, respectively. We define as stable those compositions that have lower free energy than any isochemical mixture of other compounds or pure elements. For all the newly predicted structures we computed phonons, and found them to be dynamically stable. In the entire region of explored pressures, NaCl is also a stable compound; it will not spontaneously decompose into other compounds. Thus, to obtain the newly predicted compounds, it is not sufficient merely to

[1]Department of Applied Physics, China Agricultural University, Beijing 100080, China. [2]Department of Geosciences, Center for Materials by Design, and Institute for Advanced Computational Science, State University of New York, Stony Brook, NY 11794, USA. [3]Moscow Institute of Physics and Technology, 9 Institutskiy Lane, Dolgoprudny City, Moscow Region 141700, Russia. [4]School of Materials Science, Northwestern Polytechnical University, Xi'an 710072, China. [5]Geophysical Laboratory, Carnegie Institution of Washington, 5251 Broad Branch Road NW, Washington, DC 20015, USA. [6]Center for Energy Matter in Extreme Environments and Key Laboratory of Materials Physics, Institute of Solid State Physics, Chinese Academy of Sciences, 350 Shushanghu Road, Hefei, Anhui 230031, China. [7]Center for Advanced Radiation Sources, University of Chicago, Chicago, IL 60637, USA. [8]Photon Science DESY, D-22607 Hamburg, Germany.

*Corresponding author. E-mail: zwwjennifer@gmail.com (W.Z.); artem.oganov@sunysb.edu (A.R.O.)
†These authors contributed equally to this work.

compress NaCl; one must do so at high temperatures (to overcome kinetic barriers) and with excess of either Na or Cl. Electronic densities of states (fig. S5) show that most of these compounds are poor metals, with pronounced pseudogaps at the Fermi level. Cl-rich compounds can be considered as n-type semiconductors, whereas Na-rich phases are p-type semiconductors. Pseudogaps imply an electronic mechanism of their stabilization.

At 20 to 48 GPa, $NaCl_3$ is stable in the *Pnma* structure, which has four formula units in the unit cell. Unlike all the other new phases predicted here (which are metallic), this phase is a semiconductor. Its structure (Fig. 2B) contains almost linear asymmetric Cl_3 groups. Bader analysis (*16*) shows that the middle atom in the Cl_3 group is nearly neutral, with most negative charge on the side atoms (table S1) and the total charge of this anion group is ~ –0.8. *Pnma*-$NaCl_3$ has ionic bonding between Na^+ and $[Cl_3]^-$ and rather unusual covalent bonding within $[Cl_3]^-$ groups. The latter are reminiscent of the well-known trihalide ions I_3^-, Br_3^-, and $ClICl^-$, and of the hypothetical H_3^- ion (*17*), which is predicted to have charge configuration $[H^{-0.81}H^{+0.72}H^{-0.81}]^{-0.9}$. In a Zintl-like scheme, the central Cl atom must be positively charged to be able to form two covalent bonds and satisfy the octet rule. In the valence-shell electron pair repulsion model (*18*), the central Cl atom of the Cl_3^- group adopts the dsp^3 hybridization and has five electron pairs, bringing a negative net charge and violating the octet rule. For chlorine atoms, unlike iodine, it is not easy to populate vacant d orbitals (which nicely explains the structure of $ClICl^-$ ions) and the two schemes work simultaneously; this explains the nearly zero charge of this central atom and its increased (although still relatively small) d-orbital population. At 48 GPa, this peculiar insulating ionic state breaks down, and $NaCl_3$ transforms into a metallic A15 (Cr_3Si-type) structure with space group *Pm*3*n*.

$NaCl_7$, stable above 142 GPa, has a cubic structure (space group *Pm*3; Fig. 2A) derivative of the A15 (β-W or Cr_3Si) type. The *Pm*3-$NaCl_7$ structure is obtained from *Pm*3*n*-$NaCl_3$ by substituting the central Na atom (inside a Cl_{12} icosahedron) with Cl (Fig. 2, A and C). The lattice parameters and bond lengths of $NaCl_3$ and $NaCl_7$ are very close (e.g., within 0.5% at 200 GPa) because at this pressure Na and Cl have almost identical sizes, whereas in ambient conditions Cl^- is much larger than Na^+ (ionic radii are 1.81 Å and 1.02 Å, respectively). This opens the possibility of nonstoichiometry and disorder, with the potential for Anderson localization of electronic and phonon states.

At 200 GPa, the shortest Cl-Cl distance in $NaCl_3$ is 2.06 Å, only slightly longer than the Cl-Cl bond in the Cl_2 molecule (1.99 Å). These Cl-Cl bonds form extended monatomic chains running along the three mutually perpendicular axes. This type of structure resembles a textbook linear chain with a partially filled band, which in the free state is unstable against Peierls distortion (*19*). An isolated Cl chain has a ½ filled band, and at low pressures it should break into Cl_2 molecules, but in $NaCl_3$ this band is ⅔ filled as a result of the extra electron donated by Na, and the chain should break into Cl_3^- ions, which we indeed see in the *Pnma*-$NaCl_3$ phase at lower pressures. The application of pressure and the influence of other chemical entities (Na and nonchain Cl atoms) stabilize these chains in $NaCl_3$, $NaCl_7$, and elemental chlorine. Peierls theorem also explains the results of our phonon calculations indicating that both *Pm*3*n*-$NaCl_3$ and $NaCl_7$ can exist only at high pressure and are not quenchable to atmospheric pressure.

Electronic band structures of $NaCl_3$ and $NaCl_7$ show a deep and wide pseudogap for $NaCl_3$-*Pm*3*n* (Fig. 3, A and B). In both structures, Cl atoms forming the Cl_{12} icosahedra show toroidal electron localization function (ELF) maxima (Fig. 3, C and D) corresponding to a non–closed-shell electronic configuration, whereas the Cl1 atom occupying the center of the Cl_{12} icosahedron in $NaCl_7$ has a spherical ELF maximum. Thus, Cl1 and Cl2 atoms in $NaCl_7$ have different electronic structures and play very different chemical roles. Bader analysis (table S1) confirms this and gives an unusual positive charge to the Cl1.

For the Na-rich side of the phase diagram, we predict several thermodynamically stable compounds: tetragonal Na_3Cl (space group *P*4/*mmm*), two phases of Na_3Cl_2 [tetragonal (space group *P*4/*m*) and orthorhombic (space group *Cmmm*)], and three phases of Na_2Cl—one tetragonal (space group *P*4/*mmm*) and two orthorhombic (space groups *Cmmm* and *Imma*). Most of these are layered superstructures of the CsCl-type (B2) structure, with both Na and Cl atoms in the eightfold coordination (Fig. 2). For example, Na_3Cl can be represented as a $[NaCl][Na_2][NaCl][Na_2]\ldots$ sequence of layers, and the *c* parameter of the unit cell is doubled relative to that of B2-NaCl. This and similar structures have very interesting 2D metallic features, with alternating metallic $[Na_2]$ and insulating [NaCl] layers. Na_3Cl_2 is stable above 120 GPa, and its *P*4/*m* structure can be described as a 1D-ordered (rather than layered, 2D-ordered) substitutional superstructure of the B2-NaCl structure. Compound Na_2Cl shows a more complex behavior than Na_3Cl or Na_3Cl_2. At 100 to 135 GPa, the *P*4/*mmm* structure is stable; it is also a layered B2-type superstructure. Na_2Cl is stable at 135 to 298 GPa in the *Cmmm* structure, and above 298 GPa in the *Imma* structure, with Na and Cl atoms in the 12-fold coordination in the former, and 10- and 12-fold coordination, respectively, in the latter structure (Fig. 2, H and I).

XRD measurements of Na_3Cl and $NaCl_3$ synthesized at high pressures show new Bragg peaks after laser heating. At pressures above 60 GPa,

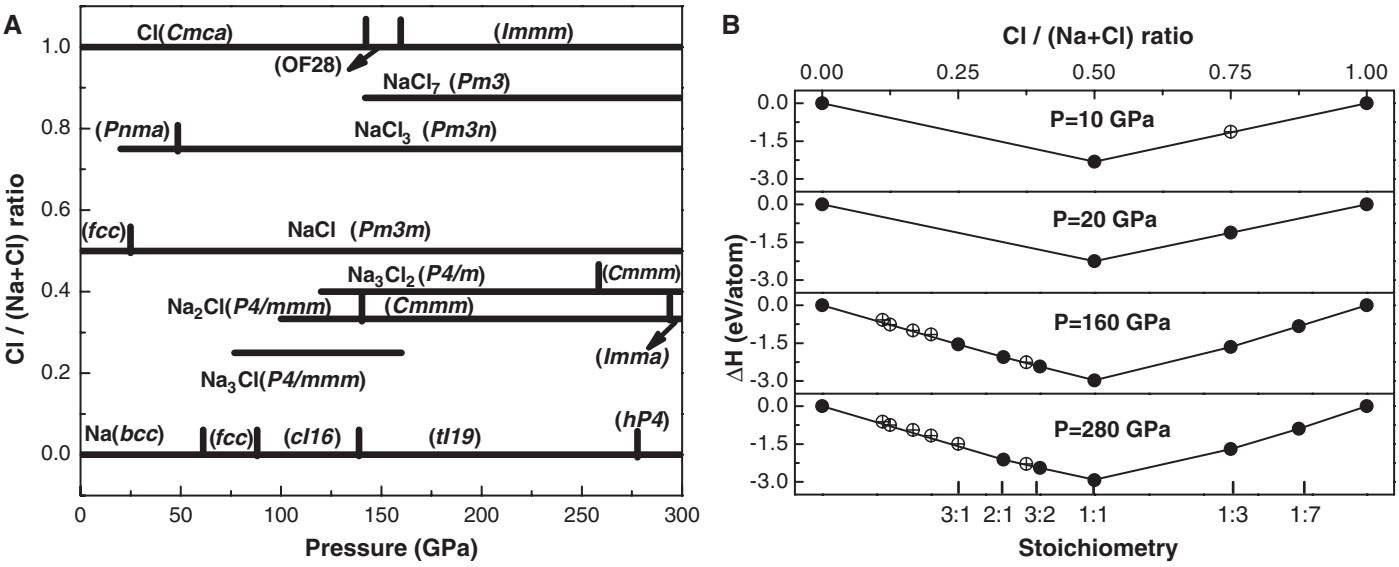

Fig. 1. Stability of new sodium chlorides. (**A**) Pressure-composition phase diagram of the Na-Cl system. (**B**) Convex hull diagram for Na-Cl system at selected pressures. Solid circles represent stable compounds; open circles denote metastable compounds. ΔH denotes the enthalpy of formation per atom.

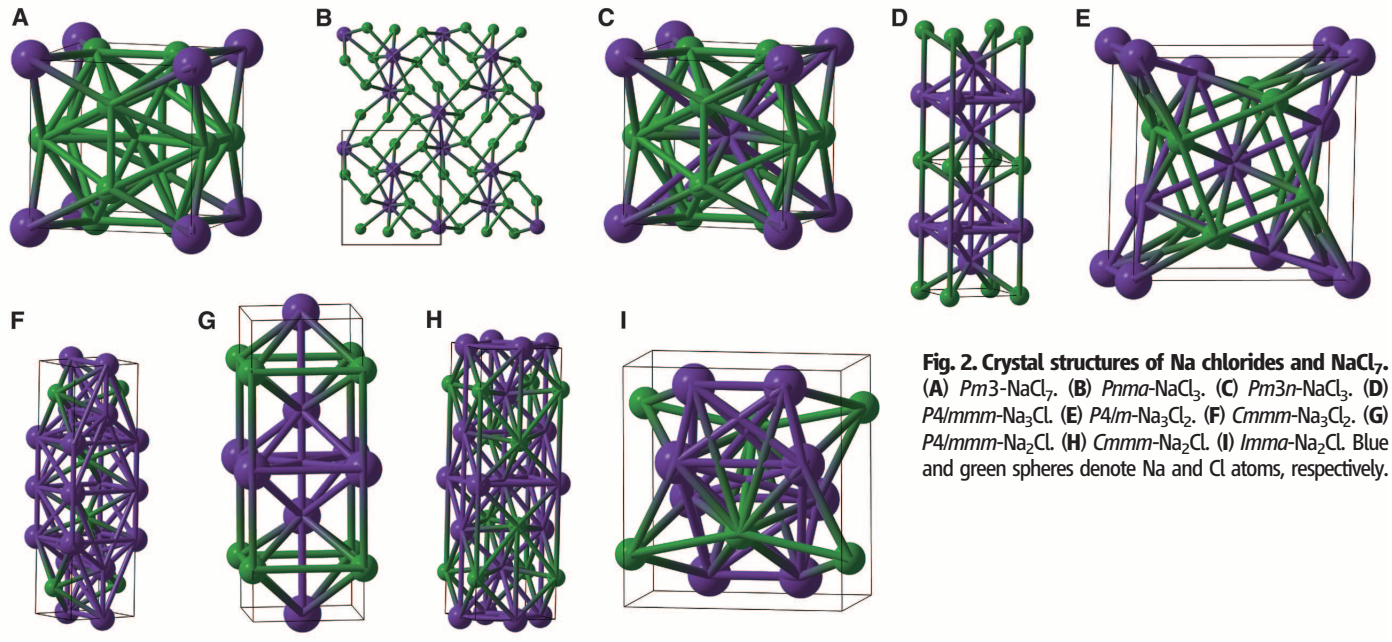

Fig. 2. Crystal structures of Na chlorides and $NaCl_7$. (**A**) *Pm*3-$NaCl_7$. (**B**) *Pnma*-$NaCl_3$. (**C**) *Pm*3*n*-$NaCl_3$. (**D**) *P*4/*mmm*-Na_3Cl. (**E**) *P*4/*m*-Na_3Cl_2. (**F**) *Cmmm*-Na_3Cl_2. (**G**) *P*4/*mmm*-Na_2Cl. (**H**) *Cmmm*-Na_2Cl. (**I**) *Imma*-Na_2Cl. Blue and green spheres denote Na and Cl atoms, respectively.

these Bragg peaks can be indexed either in a cubic $NaCl_3$ unit cell (Fig. 4A) or with a mixture of the cubic and the orthorhombic *Pnma* $NaCl_3$ unit cell. With pressure decreasing below 54 GPa, after laser heating, only the peaks of the orthorhombic $NaCl_3$ are present in the XRD patterns (fig. S7). The XRD pattern usually also contains peaks from unreacted B2-NaCl and orthorhombic chlorine, which were identified using our theoretical calculations.

From the XRD data, we obtained the lattice parameters and the unit cell volume for the two structures as a function of pressure for the decompression sequence. There is good agreement between the experimental and theoretical equations of state for both $NaCl_3$ structures (Fig. 4C). Also, in agreement with the theoretical predictions, we find that two new $NaCl_3$ phases transform from one to the other upon pressure release at 300 K, although the transition is sluggish and there is a large range of phase coexistence. *Pnma*-$NaCl_3$ remains metastable at pressures as low as 18 GPa and decomposes to NaCl and Cl_2 at lower pressures.

Raman spectroscopy of reacted Cl-rich compounds confirmed the XRD data. We observed Raman spectra of two different kinds; at some pressure and observation points, they were even superimposed. The Raman spectra of the excess Cl_2 were easy to identify because we also collected reference data for unreacted materials as a function of pressure. The Raman spectra of two polymorphic modifications of $NaCl_3$ (figs. S8 and S9) are quite different. In cubic $NaCl_3$ we observe one broad strong band near 450 cm^{-1} and a number of weaker features, whereas in *Pnma* $NaCl_3$ there are a number of narrow peaks. In both cases the agreement between theory and experiment is good concerning the major peak positions. Moreover, experimental and theoretical pressure dependences of the Raman frequencies (fig. S10) are also in good agreement for both structures. However, in cubic phase we observed a number of extra peaks (Raman-forbidden for a *Pm*3*n* lattice) corresponding to other zone-center phonons; that is, some of the selection rules appear to be lifted. These selection rules could be substantially lifted in surface Raman scattering (as happens in metals), because of disorder in site occupation or variable stoichiometry (as Cl and Na are easily interchangeable at high pressure). Optical

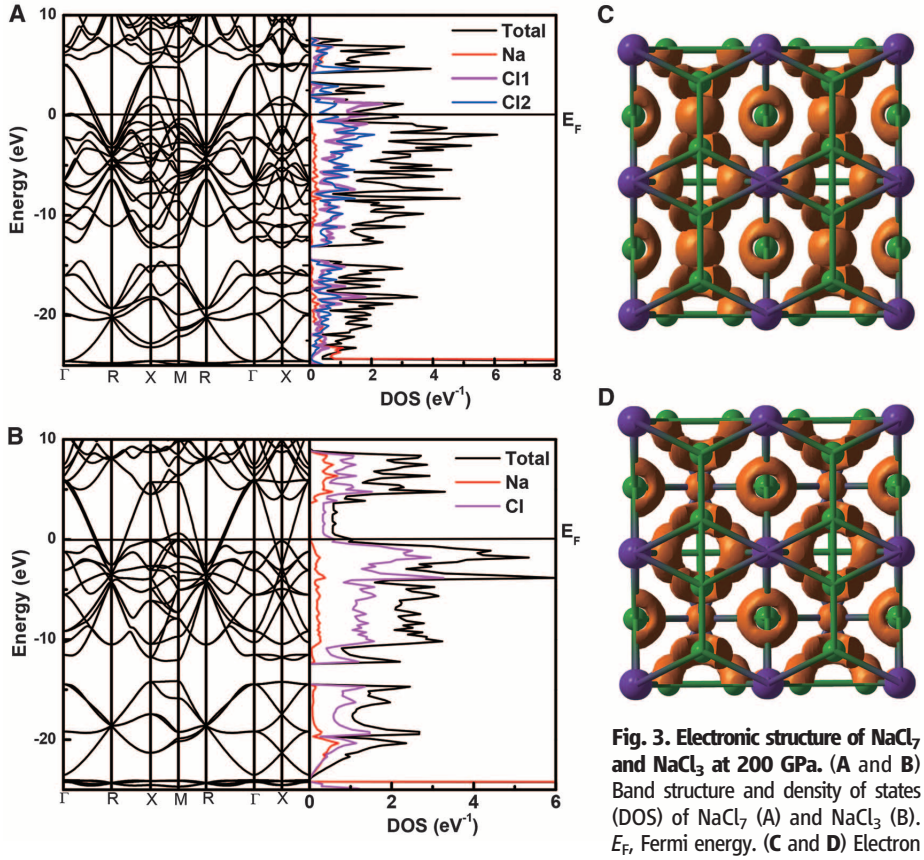

Fig. 3. Electronic structure of $NaCl_7$ and $NaCl_3$ at 200 GPa. (**A** and **B**) Band structure and density of states (DOS) of $NaCl_7$ (A) and $NaCl_3$ (B). E_F, Fermi energy. (**C** and **D**) Electron localization function of (C) $NaCl_7$ and (D) $NaCl_3$ at ELF = 0.80. For clarity, atom-projected DOSs in (A) and (B) were multiplied by 3 (for $NaCl_7$) and by 4 (for $NaCl_3$) Colors are as in (A) and (B).

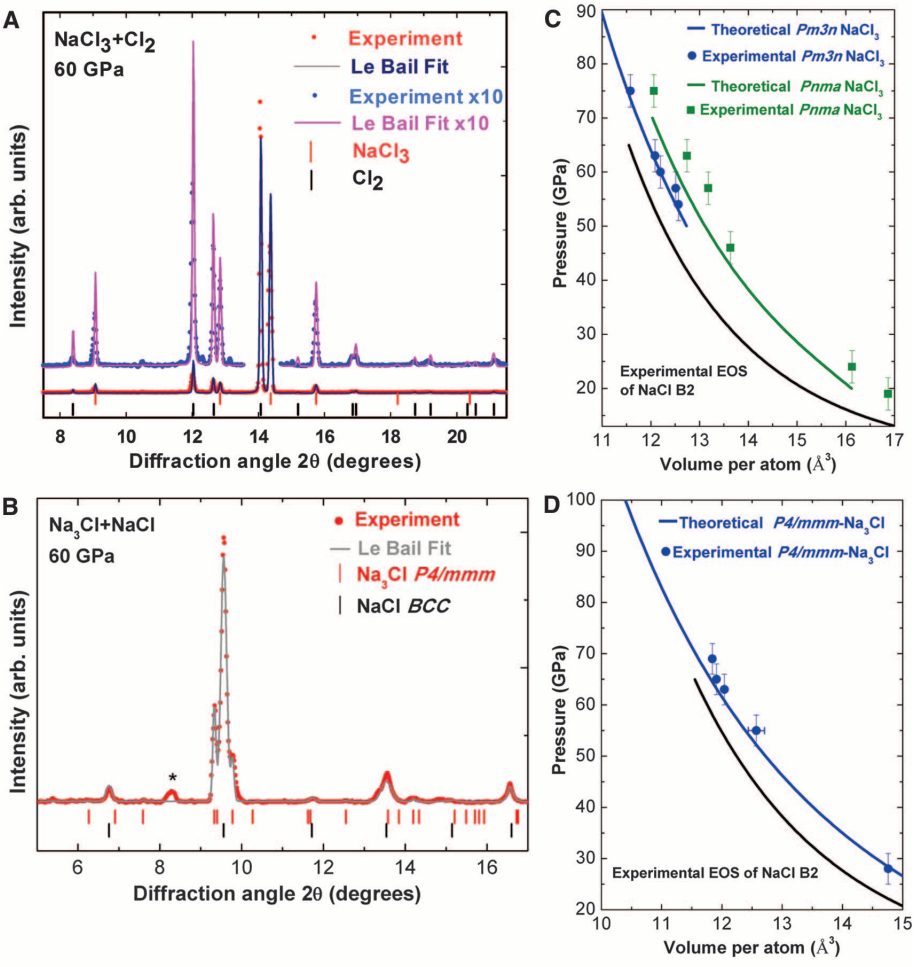

Fig. 4. Powder x-ray diffraction patterns and equations of state for $NaCl_3$ and Na_3Cl. (**A** and **B**) $NaCl_3$ in Cl_2 medium (A) and Na_3Cl in Na medium (B) collected at 60 GPa. Vertical ticks correspond to Bragg peaks of Na-Cl phases. The x-ray wavelengths are 0.5146 Å in (A) and 0.3344 Å in (B). The peak marked by the asterisk corresponds to the strongest peak of rhenium (gasket material). (**C** and **D**) Equations of state of $NaCl_3$ (C) and Na_3Cl (D) as determined experimentally (symbols) and theoretically (lines).

absorption spectra of the synthesized material (fig. S6) show a gap-like feature at 1.7 eV, which is consistent with the predicted prominent pseudogap in the electronic density of states (Fig. 3B).

The case of Na-rich material is similar but less complex. XRD of the samples laser-heated above 60 GPa showed new Bragg peaks that could be indexed in a tetragonal *P4/mmm* unit cell (Fig. 4B) across the whole pressure range of this study. The XRD pattern usually also contained peaks from unreacted cubic B1 or B2 NaCl and body-centered cubic (bcc) or face-centered cubic (fcc) sodium (*20*). The lattice parameters of new material agree well with the theoretically predicted *P4/mmm* Na_3Cl in a wide pressure range of 27 to 70 GPa (Fig. 4D). The Raman data (fig. S11) are also consistent with theoretical predictions. However, as in the case of the Cl-rich compounds, in addition to two Raman-allowed modes, we also observe a number of Raman-forbidden bands whose positions agree reasonably well with other computed zone-center phonons. Finally, Raman data show that newly synthesized Na-rich material can be (meta) stable down to 20 GPa (figs. S11 and S12) and then decomposes into NaCl and Na at lower pressures.

The theoretical prediction and experimental synthesis of unexpected chemical compounds in a simple binary system, such as Na-Cl, is not entirely unexpected. Counterintuitive compounds (such as LiH_2, LiH_6, and LiH_8) have been predicted (*21*) to appear under pressure, but experiments have so far failed to find them (*22*). Our results suggest that new stable compositions with unusual chemical bonding may exist in other simple systems, such as K-Cl, but also in important planet-forming systems such as Mg-Si-O (*23*) and H-C-N-O. Furthermore, these results point to possibilities for creating materials with unusual properties that may be quenchable to ambient conditions.

References and Notes

1. Y. Ma *et al.*, *Nature* **458**, 182–185 (2009).
2. P. Li, G. Gao, Y. Ma, *J. Chem. Phys.* **137**, 064502 (2012).
3. N. Sata, G. Y. Shen, M. L. Rivers, S. R. Sutton, *Phys. Rev. B* **65**, 104114 (2002).
4. T. Sakai, E. Ohtani, N. Hirao, Y. Ohishi, *J. Appl. Phys.* **109**, 084912 (2011).
5. D. L. Heinz, R. Jeanloz, *Phys. Rev. B* **30**, 6045–6050 (1984).
6. W. A. Bassett, T. Takahash, H.-K. Mao, J. S. Weaver, *J. Appl. Phys.* **39**, 319 (1968).
7. S. Ono, *J. Phys. Conf. Ser.* **215**, 012196 (2010).
8. S. Froyen, M. L. Cohen, *Phys. Rev. B* **29**, 3770–3772 (1984).
9. X. Chen, Y. Ma, *Europhys. Lett.* **100**, 26005 (2012).
10. M. Ross, *J. Chem. Phys.* **56**, 4651 (1972).
11. A. R. Oganov, C. W. Glass, *J. Chem. Phys.* **124**, 244704 (2006).
12. A. O. Lyakhov, A. R. Oganov, H. T. Stokes, Q. Zhu, *Comput. Phys. Commun.* **184**, 1172–1182 (2013).
13. A. R. Oganov, A. O. Lyakhov, M. Valle, *Acc. Chem. Res.* **44**, 227–237 (2011).
14. A. R. Oganov, Y. Ma, A. O. Lyakhov, M. Valle, C. Gatti, *Rev. Mineral. Geochem.* **71**, 271–298 (2010).
15. See supplementary materials on *Science* Online.
16. R. F. W. Bader, *Atoms in Molecules. A Quantum Theory* (Oxford Univ. Press, Oxford, 1990).
17. S. J. Grabowski, R. Hoffmann, *ChemPhysChem* **13**, 2286–2288 (2012).
18. R. J. Gillespie, I. Hargittai, *The VSEPR Model of Molecular Geometry* (Dover, New York, 2012).
19. R. Hoffmann, *Solids and Surfaces: A Chemist's View on Bonding in Extended Structures* (VCH, New York, 1988).
20. M. Hanfland, I. Loa, K. Syassen, *Phys. Rev. B* **65**, 184109 (2002).
21. E. Zurek, R. Hoffmann, N. W. Ashcroft, A. R. Oganov, A. O. Lyakhov, *Proc. Natl. Acad. Sci. U.S.A.* **106**, 17640–17643 (2009).
22. R. T. Howie, O. Narygina, C. L. Guillaume, S. Evans, E. Gregoryanz, *Phys. Rev. B* **86**, 064108 (2012).
23. Q. Zhu, A. R. Oganov, A. O. Lyakhov, *Phys. Chem. Chem. Phys.* **15**, 7696–7700 (2013).

Acknowledgments: Supported by the Young Teachers Development Project in China Agricultural University (W.Z.); NSF grants EAR-1114313 and DMR-1231586, DARPA grants W31P4Q1210008 and W31P4Q1310005, Government of the Russian Federation grant 14.A12.31.0003, China's Foreign Talents Introduction and Academic Exchange Program grant B08040 (A.R.O.); NSF, the Army Research Office, and EFREE, a BES-EFRC center at Carnegie (A.F.G.); and German Federal Ministry of Education and Research grant 05K10RFA (Z.K.). M.S. acknowledges support from CDAC (NNSA). Calculations were performed on XSEDE facilities (charge no. TG-DMR110058) and on the cluster of the Center for Functional Nanomaterials, Brookhaven National Laboratory, which is supported by the U.S. Department of Energy, Office of Basic Energy Sciences (DOE-BES) under contract DE-AC02-98CH10086. X-ray diffraction experiments were performed at GeoSoilEnviroCARS (Sector 13), Advanced Photon Source (APS), Argonne National Laboratory, and Petra III, DESY, Hamburg, Germany. GeoSoilEnviroCARS is supported by NSF Earth Sciences grant EAR-1128799 and DOE Geosciences grant DE-FG02-94ER14466. Use of the Advanced Photon Source was supported by DOE-BES under contract DE-AC02-06CH11357. Portions of this research were carried out at the light source PETRAIII at DESY, a member of the Helmholtz Association (HGF). USPEX code is available at http://uspex.stonybrook.edu and experimental data are available in the supplementary materials. Author contributions: A.R.O. designed the research. W.Z., A.R.O., Q.Z., and S.E.B. performed the calculations, interpreted data, and wrote the paper. A.L. wrote the latest version of the structure prediction code. A.F.G. and E.S. performed the experiments, interpreted the data and contributed in writing the manuscript. M.S., V.P., and Z.K. performed the experiments and contributed to the experimental methods.

Supplementary Materials

www.sciencemag.org/content/342/6165/1502/suppl/DC1
Materials and Methods
Supplementary Text
Figs. S1 to S12
Table S1
References (*24–32*)

21 August 2013; accepted 28 October 2013
10.1126/science.1244989